Global Journal of Engineering and Technology Advances

eISSN: 2582-5003

Cross Ref DOI: 10.30574/gjeta

Journal homepage: https://gjeta.com/

Global Journal of Engineering and Technology Advances

Global Scholar Press, INDIA

(Research Article)

FOC of Induction Motor for Elevator Application

Friday N. Chukwu, Ekom E. Okpo * and Imo E. Nkan

Department of Electrical and Electronic Engineering, Akwa Ibom State University, Mkpat Enin 1167, Nigeria.

Global Journal of Engineering and Technology Advances, 2026, 26(03), 001-013

Publication history: Received on 10 January 2026; revised on 24 February 2026; accepted on 27 February 2026

Article DOI: https://doi.org/10.30574/gjeta.2026.26.3.0043

Abstract

The demand for high-performance elevator systems in modern infrastructure requires advanced motor control strategies that ensure precise speed regulation, smooth operation, and enhanced ride comfort. Traditional control methods such as scalar control (V/f) and direct torque control (DTC) often fail to meet the stringent performance requirements of elevator applications, particularly in terms of torque ripple reduction and dynamic response. The presented study carried out an exhaustive investigation of Field-Oriented Control (FOC) enhanced with Adaptive Neuro-Fuzzy Inference System (ANFIS) controllers for induction motor drives in elevator applications. The study developed and compared three FOC control variants: conventional PI-controlled FOC, un-optimized ANFIS-based FOC, and optimized ANFIS controllers using Particle Swarm Optimization (PSO) and Genetic Algorithm (GA). A 1.1 kW three-phase induction motor was mathematically modeled and simulated in MATLAB/Simulink environment, with comprehensive data collection of 500,000 samples over a five-second simulation period. The ANFIS controllers were designed to replace conventional PI controllers in four critical control loops: speed control, flux control, d-axis current control, and q-axis current control. Performance evaluation was conducted using multiple metrics including Mean Square Error (MSE), Mean Absolute Error (MAE), Root Mean Square Error (RMSE), and coefficient of determination (R^2). Dynamic performance characteristics such as rise time, settling time, overshoot, and steady-state error were analyzed for both speed and torque responses. The results demonstrate that PSO and GA-optimized ANFIS controllers achieved superior performance in speed control, with PSO and GA variants reducing speed control error by up to 80% compared to un-optimized ANFIS, achieving zero steady-state error and the fastest dynamic response with rise times of 0.06 seconds and settling times of 0.15 seconds. However, the study revealed a critical finding that single-objective optimization significantly improved speed control performance at the expense of other control variables, highlighting the need for multi-objective strategies. While optimized ANFIS controllers excelled in speed regulation, they exhibited performance degradation in flux and current control, with some parameters showing error increases of up to 82%. Statistical analysis confirmed significant differences between optimized and un-optimized variants ($p < 0.05$), while PSO and GA-optimized controllers showed no statistically significant difference in performance.

Keywords: Field Oriented Control; Particle Swarm Optimization; Genetic Algorithm; ANFIS Controller; PI Controller

1. Introduction

The growing demand for high-speed, energy efficient, and reliable elevator drives in modern high-rise buildings has underscored the importance of advanced motor control strategies in ensuring optimal performance of vertical transportation systems [1, 2]. Among various motor control techniques, the Field Oriented Control (FOC) system approach has consistently demonstrated superior dynamic performance [3]. While Direct current machines find wide applications in industries due to design simplicity, advent in technology exposed induction motor as the best choice due to its fascinating qualities including: Robustness, efficiency and less maintenance [4, 5]. The induction motor, although a constant speed machine, must be effectively controlled to achieve the precise speed and electromagnetic torque demanded in elevator operations. Such controls ensure smooth acceleration and deceleration, reduced jerks, enhanced

* Corresponding author: Okpo E. Ekom

energy efficiency, and minimal oscillations that could in otherwise impair system performance. Traditional control strategies such as scalar control, (V/f control) and direct torque control (DTC) have been applied to elevator drives but are often limited by sluggish dynamic response and poor torque regulation. In contrast, the Field-Oriented Control (FOC) approach, originally introduced by F.Blaschke in 1971, provides superior dynamic performance and effectively addresses the shortcomings of earlier techniques [6]. Field Oriented Control (FOC) exhibits operational characteristics comparable to those of separately excited direct current (DC) machines, providing superior dynamic response, enhanced efficiency, and smoother operation. Within FOC- based induction motor systems, controllers such as the proportional (P), proportional integral (PI), and proportional integral derivative (PID) controllers play a vital role in shaping motor behavior by ensuring appropriate adjustments to real-time load variations and environmental changes. The widespread use of PI controllers, in particular, stems from their simplicity and effectiveness, making FOC especially suitable for elevator drive applications [7]. Direct torque control (DTC) and FOC delivers high dynamic performance with minimal disturbances, sensor less controls techniques on the other hand eliminates the use of feedback sensors with the aid of estimators and observers hence less tuning of PI controllers and reduction in cost of procurements [8]. Conventional motor control techniques often experience performance degradation due to their dependence on complex mathematical models and the sensitivity of motor parameters to variations. To overcome these limitations, recent achievements have introduced artificial intelligence based control strategies that significantly improve the performance of induction motors in applications such as elevators, electric vehicles, robotics, and servo systems. This technological progress represents a paradigm shift in modern machine control [9, 10]. The presented study is therefore significant as it will present a novel strategy to enhance the performance of induction motor for varying applications by investigating the performance metrics of three variants controllers including: PI controller, Un-optimized ANFIS, and optimized ANFIS controller using conventional PI-FOC as the baseline for comparative purpose. The study in [11, 12] investigated slip ring induction motor (SRIM) control using a dual Field Oriented Control (FOC) configuration based on superposition principle, where the total developed power equates to the sum of the individual contributions from each configurations were successfully combined, validated through simulation and experimental studies, the analysis did not adequately address the implications of this dual strategy on the performance, reliability, and responsiveness of induction motors in critical applications such as elevators, cranes, and electric vehicles, where precise speed and torque regulation are essential. The study in [13] proposed a genetic algorithm-based hybrid fuzzy-fuzzy controller (GA-HFFC) integrated with space vector pulse width modulation (SVPWM) for variable speed induction motor (IM) drives. By leveraging stator current and supply frequency, this approach demonstrated improved performance and adaptability under diverse load and operating conditions, offering a potential solution to some limitations of conventional FOC systems. However, despite its robustness, the GA-HFFC was found to lack real time computational capability under highly dynamic conditions, which remains a significant challenge in practical applications. The study in [14] deployed advanced deep reinforcement learning (DRL) to address the complex dynamic behavior and external disturbances in induction machines, a challenge for conventional linear controllers. The approach showed strong adaptability; however, its performance declined under highly dynamic operating conditions and increased efficiency requirements. MATLAB/Simulink simulation was conducted in [15] to enhance the dynamic response of an induction motor by incorporating the super-twisting algorithm and synergetic control into the conventional frame work. This integration effectively minimized torque ripple, flux oscillations, total harmonic distortion (THD), and speed disturbances, delivering improved performance and robustness compared to the traditional FOC method. Nonetheless, the approach exhibited limited adaptability under real-world dynamic operating conditions. In addressing the identified gaps in the reviewed works, a comparative study with three variants controllers under identical conditions using PI controllers as the baseline for comparison were deployed to evaluate the characteristics performance of induction motor tailored to elevator system applications. The remaining portion of this paper is organized as follows. Section II explains the dynamic modelling of the induction motor with PI-FOC system, section III covers the proposed un-optimize ANFIS controller and the algorithmically improved ANFIS controllers, section IV covers the simulation results and discussions while section V presents the conclusion.

2. Method

This section covers the systematic approach deployed to conduct comparative analysis of the dynamic performance characteristics of induction motor under Field-Oriented Control (FOC) using optimally trained Adaptive Neuro-Fuzzy Inference System (ANFIS) controllers, in contrast to conventional PI-FOC system specifically tailored for elevator applications.

2.1. Dynamic modelling of the induction motor

The dynamic modelling of the three phase induction motor follows the standard electromechanical design techniques considering the d-q axis representation in a synchronously rotating frame as the reference axis, the motor is symmetrical with balance 3-phase input voltages. Core parameters of the induction motor were identified and their specifications used in the dynamic modelling of the induction motor. The dynamic modelling commenced with representation of the stator and rotor voltage equations as studied in [7], the stator quadrature voltage (V_{qs}) is expressed as:

$$V_{qs} = r_s i_{qs} + w\lambda_{ds} + d/dt(\lambda_{qs}) \quad (1)$$

Where, r_s is the stator resistance, i_{qs} is the stator quadrature current, w is the motor angular velocity, λ_{ds} is the stator direct axis flux linkage, and λ_{qs} is the stator quadrature flux linkage. The stator direct axis voltage V_{ds} is presented in Eqn. 2 as:

$$V_{ds} = r_s i_{ds} - w\lambda_{qs} + d/dt(\lambda_{ds}) \quad (2)$$

While the zero sequence component voltage is given by the following expression in Eqn. 3:

$$V_{0s} = r_s i_{0s} + d/dt(\lambda_{0s}) \quad (3)$$

Where i_{0s} is defined as the zero sequence stator current and λ_{0s} is the zero sequence flux linkage . The rotor quadrature voltage (V_{qr}) is defined by the following combination:

$$V_{qr} = r_s i_{qr} + (\omega - \omega_r)\lambda_{dr} + d/dt(\lambda_{qr}) \quad (4)$$

Where, i_{qr} is the rotor quadrature current, w_r is the rotor angular velocity, λ_{dr} is the rotor direct axis flux linkage, and λ_{qr} is the rotor quadrature flux linkages. The rotor direct axis voltage V_{dr} of the induction motor is given in Eqn. 5 as:

$$V_{dr} = r_s i_{dr} - (\omega - \omega_r)\lambda_{dr} + d/dt(\lambda_{qr}) \quad (5)$$

Where I_{dr} is defined as the rotor direct axis current and ω_r represent the rotor angular velocity.

$$V_{dr} = r_s i_{dr} - (\omega - \omega_r)\lambda_{qs} + d/dt(\lambda_{dr}) \quad (6)$$

The zero sequence rotor voltage of the induction motor is represented by the following expression:

$$V_{0r} = r_s i_{0r} + d/dt(\lambda_{0r}) \quad (7)$$

Presented in Eqn. 8 to Eqn.11 are the induction motor flux linkages in both the stator and rotor sides as studied in [16], with the stator quadrature flux linkage (λ_{qs}) expressed in Eqn.8 as:

$$\lambda_{qs} = (i_{qs}L_s + L_m i_{qr}) \quad (8)$$

Where, L_s is defined as the stator inductance of the induction motor, and i_{qr} represent the rotor quadrature current. The direct axis flux linkage λ_{ds} is represented by the combination in Eqn. 9:

$$\lambda_{ds} = (i_{ds}L_s + L_m i_{dr}) \quad (9)$$

The flux linkage for the rotor quadrature and direct axis are represented by the combination of the following mathematical expressions:

$$\lambda_{qr} = (i_{qr}L_r + L_m i_{qs}) \quad (10)$$
$$\lambda_{dr} = (i_{dr}L_r + L_m i_{ds}) \quad (11)$$

The stator quadrature current is derived by substituting Eqn. 8 and Eqn. 9 into Eqn.1 given as follows:

$$i_{qs} = \int (1/L_s)(V_{qs} - i_{qs}r_s - \frac{L_m d}{dt(i_{qr})} - \omega L_s i_{ds} - \omega L_m i_{dr}) \quad (12)$$

Substituting Eqn. 8 and Eqn. 9 into Eqn. 2 yields the stator direct axis current (i_{ds}) of the induction motor given as follows:

$$i_{ds} = \int (1/L_s)(V_{ds} - i_{ds}r_s - \frac{L_m d}{dt(i_{dr})} + \omega L_s i_{qs} + \omega L_m i_{qr} \quad (13)$$

The rotor quadrature axis current (i_{qr}) of the induction motor was derived by substituting Eqn. 8 and Eqn. 9 into Eqn. 4 as represented by the expression in Eqn. 14:

$$i_{qr} = \int \left(\frac{1}{L_r}\right)(V_{qr} - i_{qr}r_r - \frac{L_m d}{dt(i_{qs})} - \omega L_r i_{dr} - \omega L_m i_{ds}) \quad (14)$$

The rotor direct axis current is expressed by combining Eqn. 8 and Eqn. 9 into Eqn. 6 to arrive at Eqn. 15:

$$i_{dr} = \int (1/L_r)(V_{qr} - i_{dr}r_r - \frac{L_m d}{dt(i_{ds})} + \omega L_r i_{qr} + \omega L_m i_{qs} \quad (15)$$

The electromagnetic torque of the induction motor is expressed by the following combination of equations:

$$T_e = (3/2)(P/2)L_m(i_{qs}i_{ds} - i_{ds}i_{qr}) \quad (16)$$

While the motor speed is represented in Eqn.17 as.

$$W_r = \int (T_e - T_l)\frac{P}{2J} \quad (17)$$

Where T_e is the electromagnetic torque, T_l is the load toque, P is the number of pole pairs and J is the motor moment of inertia. The presented systems of equations above were used for complete modelling of the induction motor in MATLAB Simulink software.

2.2. FOC-system controller structure

The FOC system consist of four distinct controllers: the speed controller, d-axis current controller, q-axis current controller, and flux controller. The speed error generated from the speed controller was used to regulate the motor's dynamic response. The flux controller achieved by combining PI controller with a summation block generated the reference quadrature current (iq_{ref}). Similarly, the q-axis current controller modeled with PI controller and a summation block gave the q-axis voltage control signal, and finally the d-axis controller modeled in similar manner generated the d-axis voltage control signal as output. All the required signals within the system were appropriately labeled for proper analysis and training of the ANFIS model. Presented in Figure 1 is the Simulink model of the Induction motor with PI controllers.

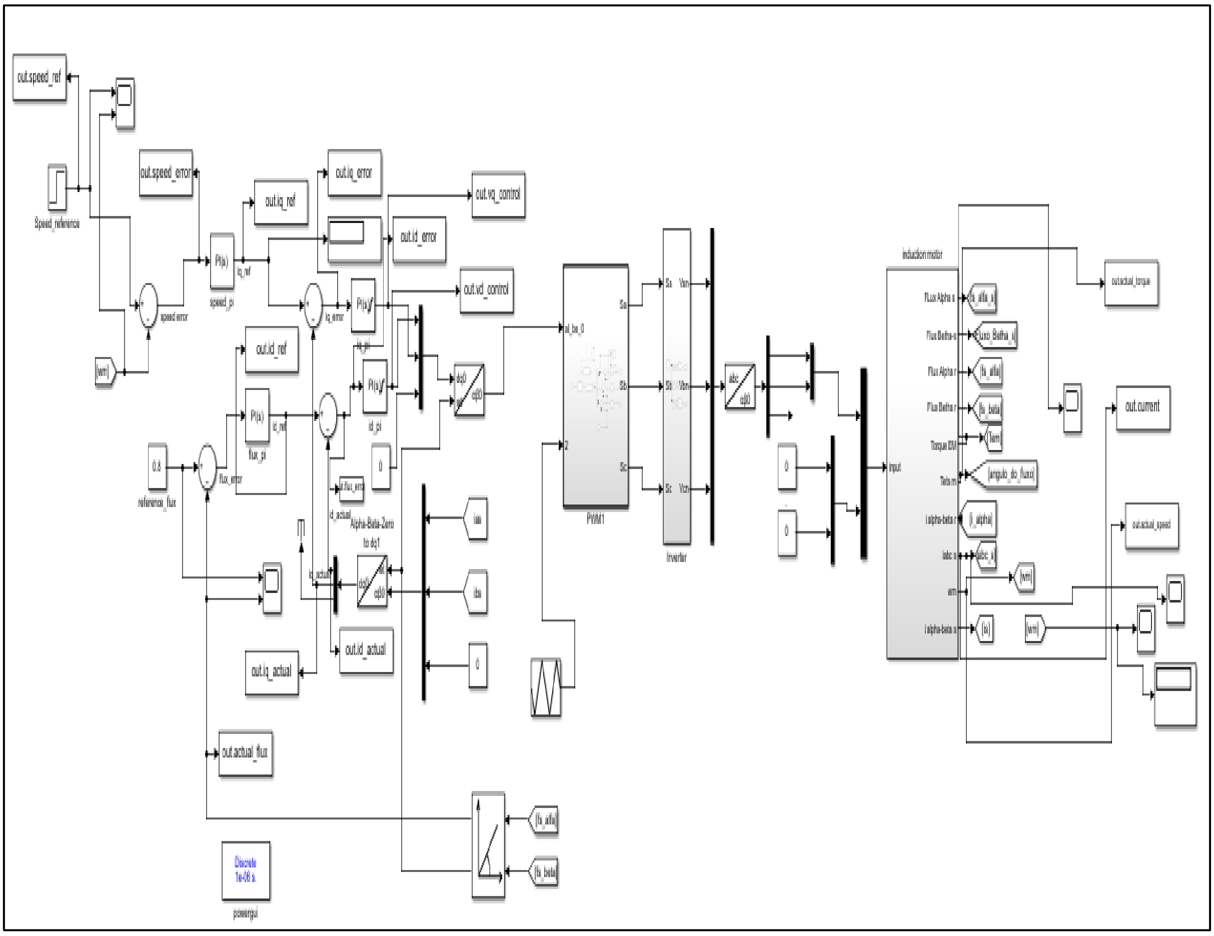

Figure 1 Model of the induction motor with PI-FOC system

3. Proposed FOC control system

This section covers the systematic approach deployed in modelling the un-optimized ANFIS and algorithmically improved ANFIS models used to replace the PI controllers along the major four loops of the FOC system.

3.1. UN-optimize ANFIS-FOC control system

The conventional PI controller along the four major loops were replaced with ANFIS controllers, this replacement was necessary to enable an easy adaptation to parameter variations and nonlinear elevator loads without requiring exact mathematical tuning. Each ANFIS was setup with three gbell membership functions, the ANFIS combines fuzzy logic to handle uncertainties/nonlinearities and neural network learning that has a self-tuning capability. Three membership functions(mf) were chosen to balance model expressiveness and computational efficiency, few mfs will reduce control precision, while too many would increase complexity and risk overfitting. Figure 2 shows the Simulink model in which all PI controllers were replaced with corresponding ANFIS-based controllers.

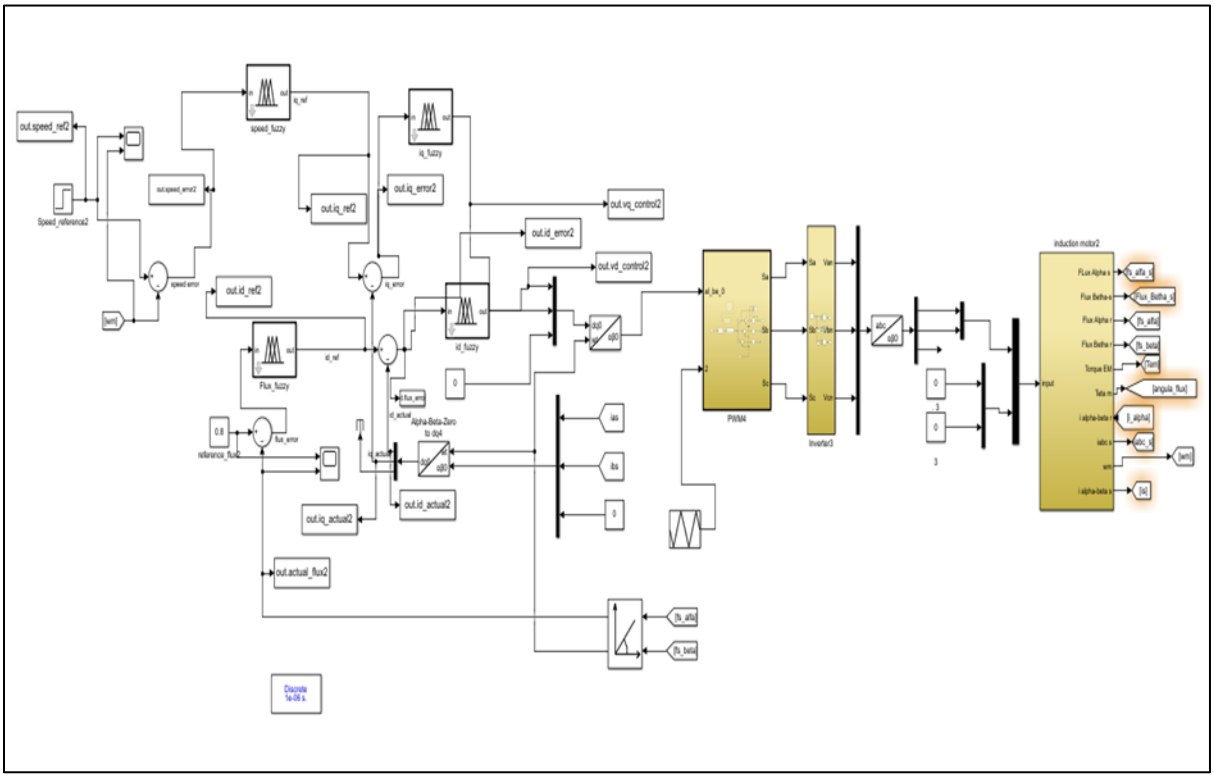

Figure 2 Induction motor ANFIS based FOC system

3.2. Proposed GA and PSO algorithm

The ANFIS model involves numerous parameters making the tuning process complex when conventional gradient-based methods are employed, this approach is prone to minima and slow convergence. To overcome these limitations, two metaheuristic optimization techniques were used to fine-tune the ANFIS parameters including: Particle Swam Optimization (PSO) and Genetic Algorithm (GA). These algorithms optimized ANFIS controller parameters for better dynamic response with major impact on the induction motor speed control. PSO algorithm mimics bird flocking/ fish schooling behavior, it was chosen because of the ability to converge faster towards optimal solutions, non-reliance on gradient information, and its capability of not getting stuck in poor local minima. Similarly, GA mimics natural evolution through selection, crossover, and mutation, it was also chosen because of its ability to explore a broader solution space and handle complex nonlinear functions. Both are population-based optimizers, making them well-suited for multidimensional search space of ANFIS parameters. PSO swarm size was set to 30 particles and maximum iteration to 100 so as to provide a balance between convergence speed and computational load. Cognitive coefficients c1 and c2 were set to 1.5 each to indicate equal weight to self-learning and social learning. The inertia weight (ω) was set to 0.7 and velocity clamping set to enabled so as to prevent divergence. The population size of GA was set to 50, crossover probability set to 0.8, mutation rate set to 0.1, maximum generation set to 100 and selection mode set to tournament selection. The GA population size was set larger than PSO to foster a more significant difference, its high crossover probability encourages exploration, while moderate mutations prevents premature convergence

4. Simulation results and discussion

The data utilized in modelling the three phase, 1.1 kW Induction motor was shown in Table 1 as follows:

Table 1 Parameters of the induction motor

No	Parameter	Specification
i	Nominal power	1.1 kW
ii	Phase voltage	220 V
iii	Moment of inertia	0.045 kgm^2
iv	Nominal frequency	60Hz
v	Number of pole pairs	2
vi	Mutual inductance (Lm)	191.7e^-3 H
vii	Stator inductance	201e^-3H
viii	Rotor inductance (Lr)	201e^-3H
ix	Stator resistance (Rs)	1Ω
x	Rotor resistance (Rr)	3.1322 Ω
xi	Stator nominal flux (Sf)	0.825 Wb
xii	Nominal torque	16Nm

The performance metrics presented in Table 2 highlights a critical insight that while optimization techniques such as (PSO and GA) significantly enhance certain aspects of ANFIS controller performance demonstrated by up to an 80% reduction in speed control error they fundamentally expose the limitations of single-objective optimization in multiple interdependent control variables. The un-optimized ANFIS, despite having higher overall errors, maintained a more uniform performance across all control variables. In contrast, the optimized variants achieved superior speed control but exhibited substantial deterioration in flux and current control accuracy. The performance metrics of the three variant controllers was shown in Table 2 as follows:

Table 2 Performance analysis of the three variants controllers

Controller	Un-MSE	PSO-MSE	GA-MSE	UN-MAE	PSO-MAE	GA-MAE	UN-R^2	PSO-R^2	GA-R^2
Speed	0.1286	0.0257	0.0257	0.3586	0.1604	0.1604	-14823.0561	-2966.6018	-2966.6018
Flux	0.0384	0.0503	0.0503	0.1946	0.2232	0.2232	-92.6581	-121.6042	-121.6042
Id	0.0952	0.1226	0.1226	0.3039	0.3494	0.3494	0.1899	-0.0438	-0.0438
Iq	0.0336	0.0610	0.0610	0.1570	0.2241	0.2241	-0.2733	-1.3144	-1.3144

Shown in Figure 3 is the graphical representation of the performance metrics of the three variants controllers corresponding to data presented in table 2 above.

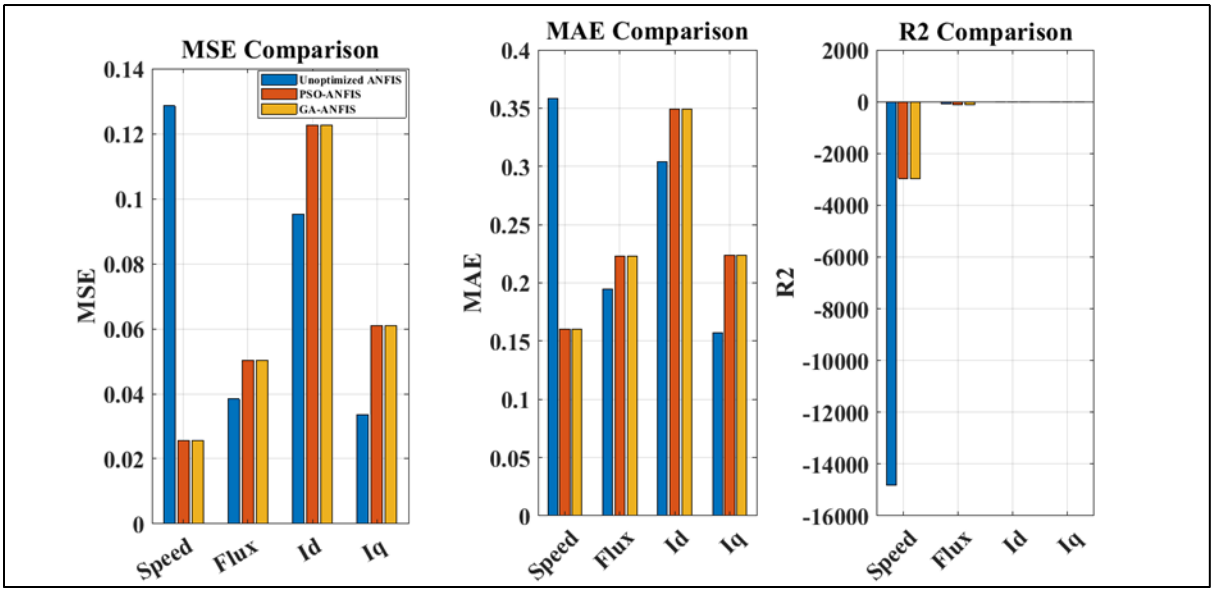

Figure 3 Performance metrics of different controllers

The graphical plots in Figure 4 showed the actual motor system responses by demonstrating the reference trajectories and system behavior that the controllers are attempting to track. The actual speed shows a step response starting from zero and reaching approximately 50 rad/s at t = 0.5 seconds, then jumping to 100 rad/s at t = 1 s, maintaining this level throughout the remaining simulation time. The actual flux exhibits a rapid rise to 0.5 wb within the first 0.1 seconds and remains relatively stable with minor fluctuations around this set point up to 0.8 wb. The actual torque displays a gradual increase from zero, reaching approximately 200 Nm by t = 1 s, then continuing to rise more gradually to about 800 Nm by the end of the 5 second simulation, representing the load characteristics that the motor system must handle.

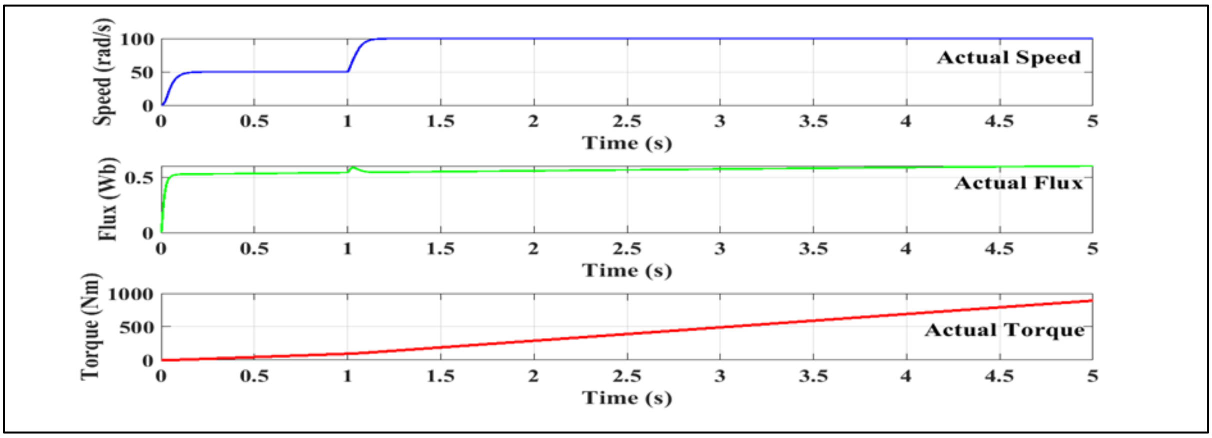

Figure 4 Graphical plots of actual motor system responses

The performance comparison between PI controller versus un-optimized ANFIS reveals significant differences in tracking capability across the four major control loops. As shown in Figure 5 in the speed controller subplot, both controllers show similar performance during steady-state operation, but the un-optimized ANFIS exhibits slightly higher reference current spikes during transients, with test data RMSE and MAE both at 0.3586. The flux controller comparison shows the PI controller and un-optimized ANFIS following nearly identical trajectories with minimal deviation, achieving test data RMSE of 0.1960 and MAE of 0.1946. For the Id controller, both controllers maintain near-zero control voltages with occasional small transients, with the un-optimized ANFIS showing test RMSE of 0.3085 and MAE of 0.3039. The Iq controller demonstrates the most significant activity during the initial transient period around t = 1 s, where both controllers generate control voltages up to 50 V, with the un-optimized ANFIS achieving test RMSE of 0.1832 and MAE of 0.1570.

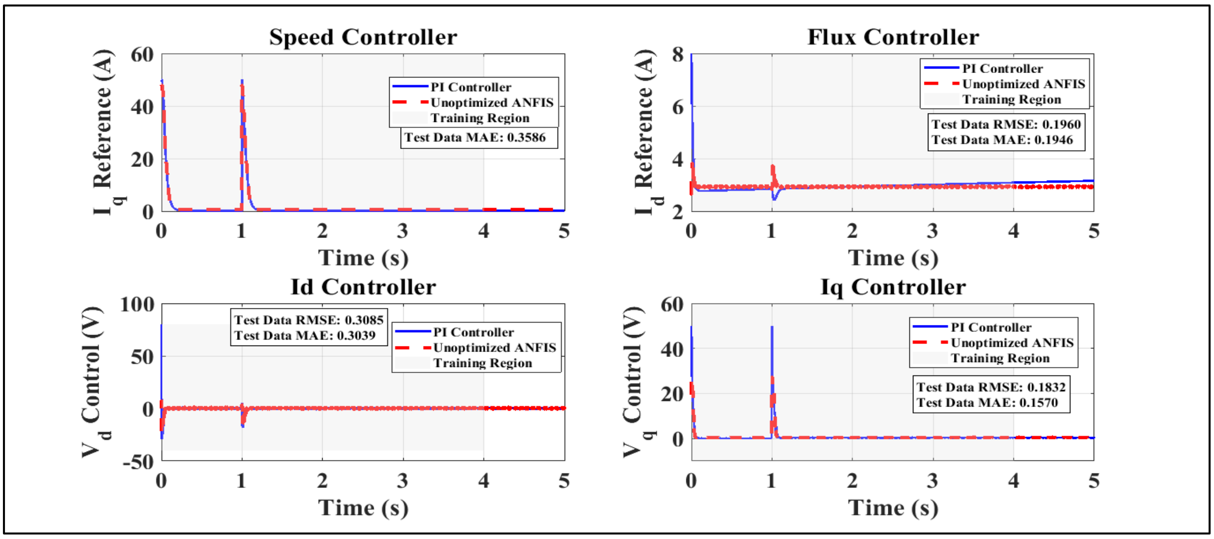

Figure 5 Performance comparison of PI-Controller vs Un-optimized ANFIS

Comparative analysis carried out on all controllers including: PI, un-optimized ANFIS, PSO-optimized ANFIS, and GA-optimized ANFIS shows important insights into the optimization effects discussed in Table 2 above. The speed controller subplot confirms that while the un-optimized ANFIS had an RMSE of 0.3586, both PSO and GA optimization reduced this to 0.1604, representing significant improvement in speed control performance. However, the flux controller comparison reveals the concerning trend where optimization degraded performance, with the un-optimized ANFIS achieving 0.1960 RMSE while both PSO and GA variants increased this to 0.2242. The Id controller shows a similar deterioration pattern, with the un-optimized version achieving 0.3085 RMSE compared to 0.3502 for both optimized variants. Most dramatically, the Iq controller demonstrates the severe performance degradation discussed earlier, where the un-optimized ANFIS achieved 0.1832 RMSE but optimization pushed this to 0.2470 for both PSO and GA variants, visually confirming the table data that showed optimization's detrimental effect on current control performance while achieving gains only in speed control as shown in the following figure.

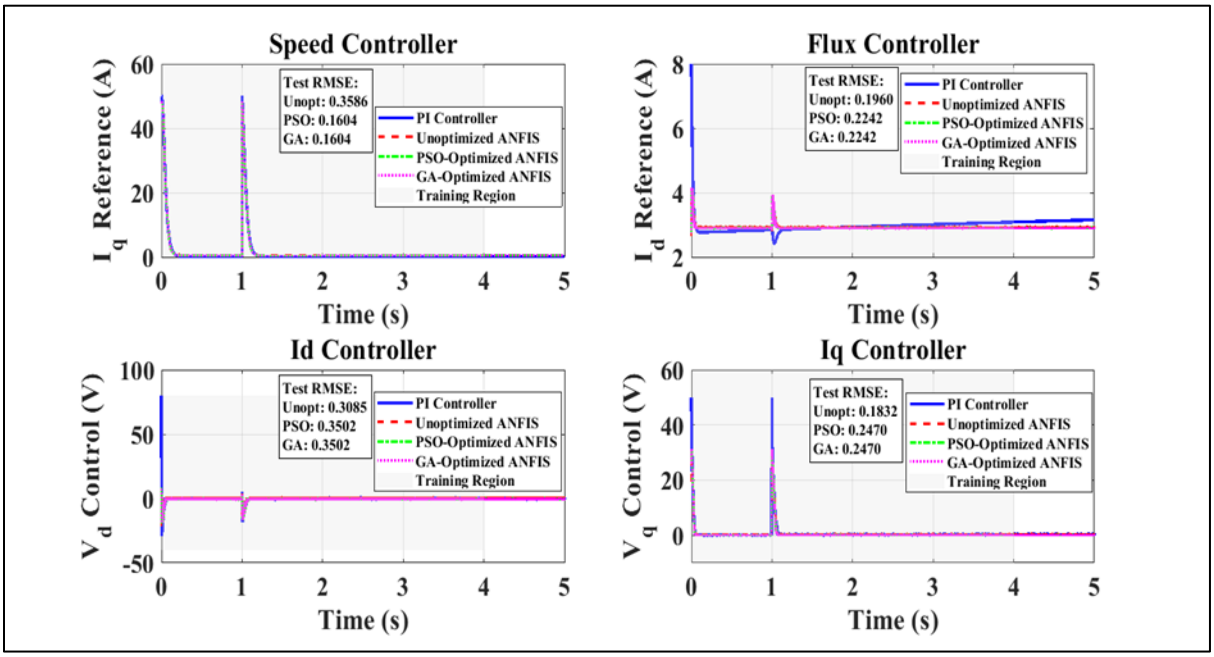

Figure 6 Comprehensive ANFIS performance comparison

In terms of error analysis, the speed controller shows successful optimization with sustained error reduction throughout the simulation period, while the flux, Id, and Iq controller errors reveal persistent degradation across the complete time horizon. Critically, these error plots expose that the optimization algorithms created controllers that maintain consistently higher error levels in three out of four control variables for the entire simulation, indicating fundamental structural changes to the ANFIS rather than temporary tuning issues. Presented in Figure 7 is the graphical plots of error analysis comparing the performance of the four controllers

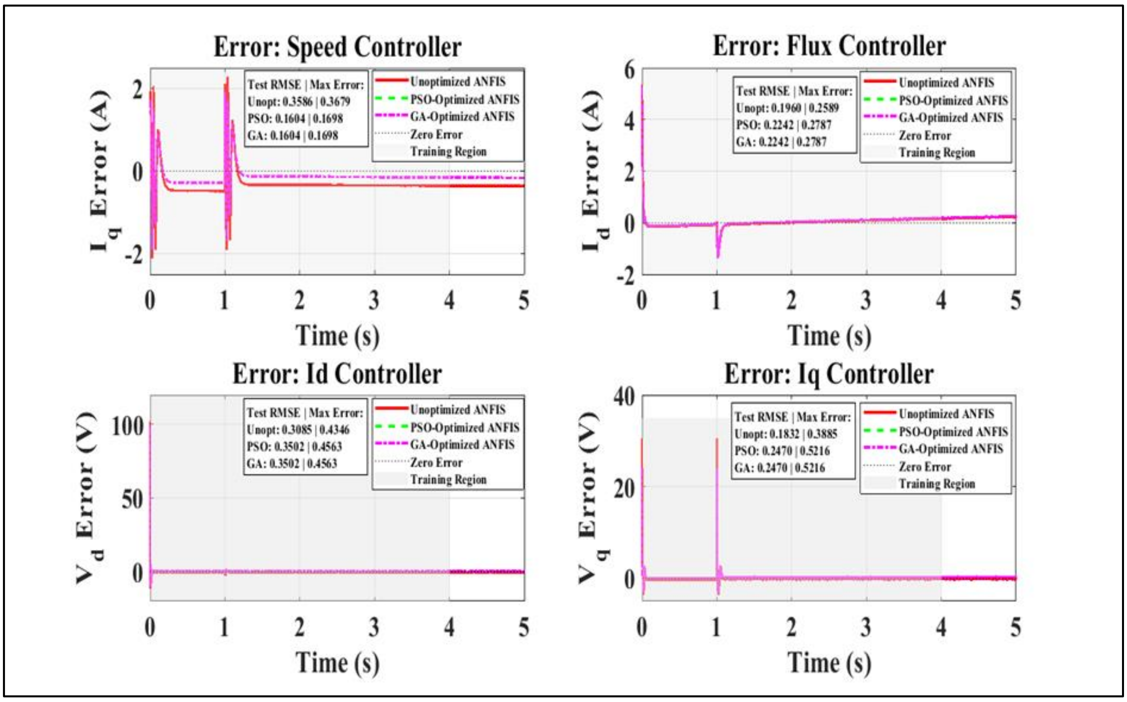

Figure 7 Comprehensive error analysis of all ANFIS methods

Investigation on the controller output response as shown in Figure 8 over the final second of simulation (4-5 seconds) reveals distinct behavioral patterns during steady-state operation. The speed controller comparison shows that while the PI reference maintains a steady value around 0.58, the un-optimized ANFIS operates at a lower level near 0.22, with both PSO and GA optimized variants tracking closer to 0.4, indicating different control strategies for maintaining the same speed set point. The flux controller comparison demonstrates all variants operating within a narrow band around 2.9-3.15, with the PI controller showing a gradual upward trend while ANFIS variants remain more stable. The Id controller comparison reveals significant control activity with all controllers oscillating between -2 to +1, suggesting ongoing regulation efforts, while the Iq controller comparison shows the most complex behavior with control outputs spanning from 0 to 0.8 and exhibiting high-frequency switching patterns across all controller types.

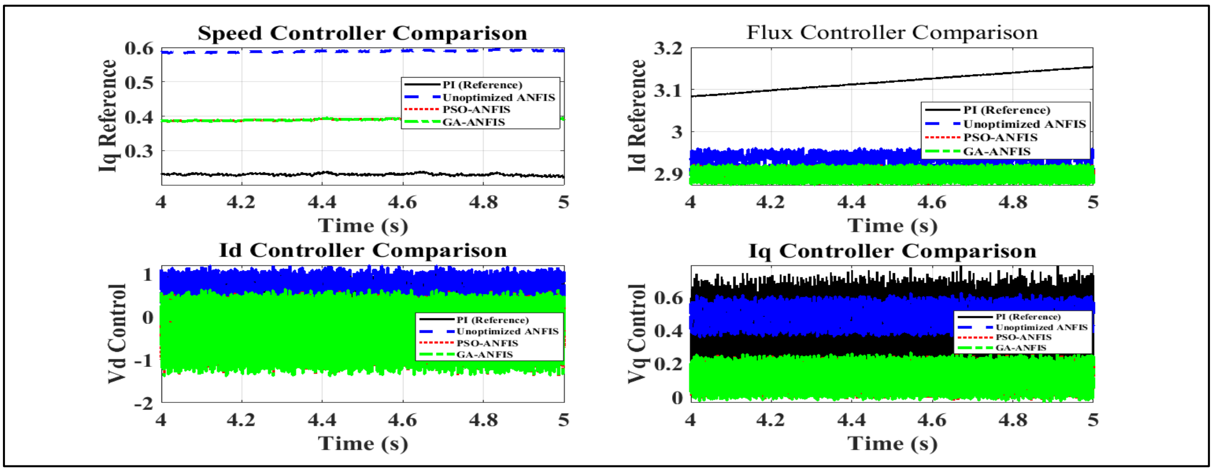

Figure 8 Controller output comparison over final second simulation time

Comparison of the dynamic behavior of the speed response during the initial transient period reveals three distinct performance characteristics. The PI controller demonstrates the slowest rise time, reaching the vicinity of the 100 rad/sec set point at 0.20 seconds, but it overshoots before reaching the target speed, as evidenced by its initial rapid ascent that exceeds the optimal trajectory. The un-optimized ANFIS (un-tuned variant) shows a more controlled response that doesn't have as much overshoot compared to the PI controller, following a smoother and more gradual approach to the 100 rad/sec set point with a rise time of 0.18 seconds. After optimization through PSO and GA fine-tuning, the overshoot was further reduced, with both optimized variants demonstrating even more controlled responses that minimize the overshoot behavior while maintaining consistent tracking performance between the two optimization methods. This progression clearly shows that while un-optimized ANFIS provides better overshoot control, the optimization process successfully further reduces this overshoot, creating increasingly stable and well-damped responses through the tuning process, though all ANFIS variants trade some response speed for superior overshoot management compared to the PI controller. Shown in Figure 9 are the dynamic speed responses of the controllers.

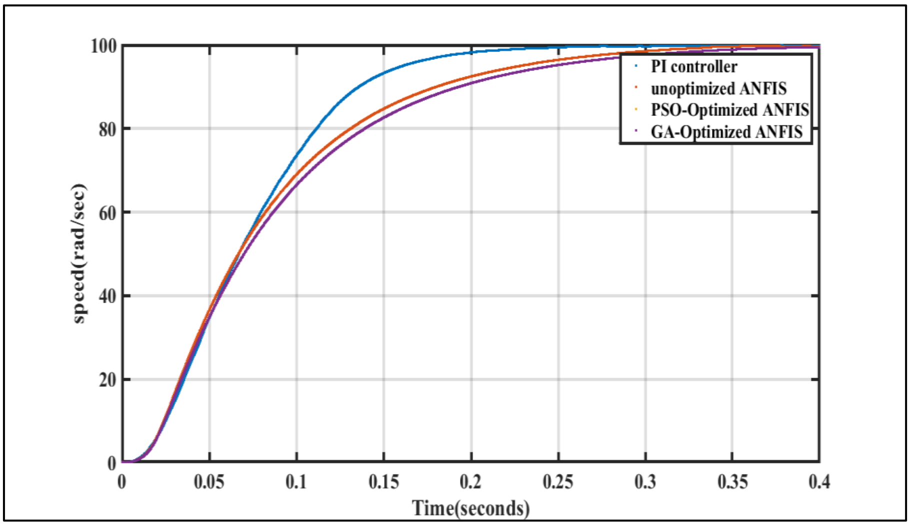

Figure 9 Comparison of ANFIS speed controller's performance

The dynamic behavior of the electromagnetic torque as shown in Figure 10 during initial transient period (0-0.4 seconds) reveals that all controller variants achieve nearly identical torque tracking performance, with peak torques reaching 55-57 Nm at 0.04 seconds before settling toward zero by 0.4 seconds. The PI controller exhibits slightly more oscillatory behavior during the decay phase with distinctive ripples, while all ANFIS variants (un-optimized, PSO, and GA) demonstrated remarkably similar and smoother torque profiles, suggesting that torque control is a strength of ANFIS architecture regardless of optimization status and can lower energy consumption, reduce thermal stress on motor components, and extend system lifespan.

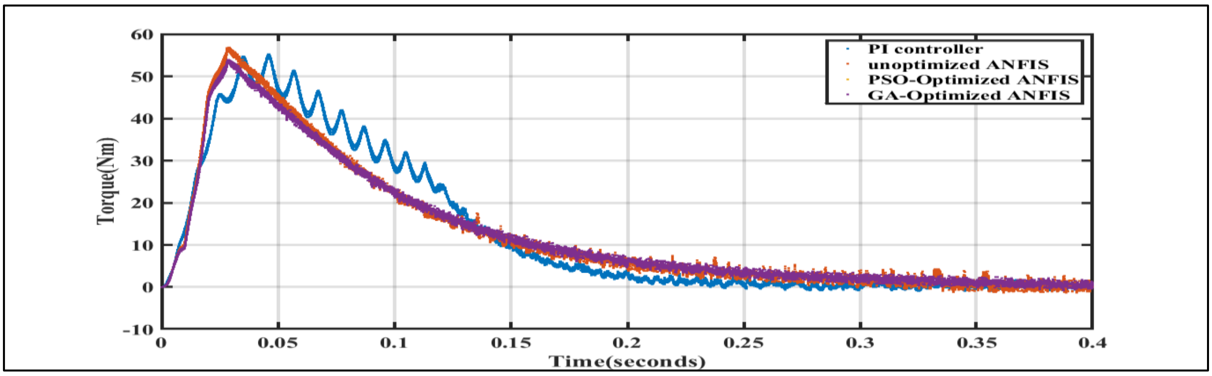

Figure 10 Comparison of torque response for the controllers

Abbreviations

ANFIS	Adaptive Neuro Fuzzy Inference System
DTC	Direct Torque Control
D-axis	Direct axis
D.C	Direct Current
DRL	Deep Reinforcement Learning
FOC	Field Oriented Control
GA	Genetic Algorithm
GA-HFFC	Genetic Algorithm Hybrid Fuzzy Fuzzy Controller
Id-Controller	Direct Axis Current Controller
Iq-Controller	Quadrature Axis Current Controller
MAE	Mean Absolute Error
MSE	Mean Square Error
Q-axis	Quadrature axis
RMSE	Root Mean Square Error
SRIM	Slip Ring Induction Motor
SVPWM	Space Vector Pulse Width Modulation
THD	Total Harmonic Distortion
PSO	Particle Swarm Optimization
PID	Proportional Integral Derivative Controller
MF	Membership Function

5. Conclusion

This study evaluated three ANFIS-based FOC control variants including un-optimized, PSO-optimize, and GA optimized ANFIS using simulation dataset of 500,000 samples. Comparative analysis carried out using conventional PI-FOC as baseline demonstrated that the optimized ANFIS controllers significantly improved speed regulation, while all ANFIS variants (un-optimized, PSO, and GA) demonstrated remarkably similar and smoother torque profiles, suggesting that torque control is a strength of ANFIS architecture regardless of optimization status. RMSE evaluation and statistical hypothesis testing confirmed superior precision and stability of both PSO and GA-optimized ANFIS controllers, with no significant difference observed between them, but a clear performance gap compared to the un-optimized variant. These findings highlight the capability of optimized ANFIS controllers to be the stringent demands of elevator drive applications, where reliability, passenger comfort, and safety are critical. However, observed trade-offs underscore the need for further exploration of multi-objective optimization strategies to balance primary control performance with secondary objectives, ensuring a more holistic and robust control solution.

Compliance with ethical standards

Disclosure of conflict of interest

The Authors proclaim no conflict of interest.

Author's contributions

Chukwu N. Friday was responsible data curation, investigations, formal analysis and writing of original draft, review, and editing.

Okpo E. Ekom and Nkan E. Imo were responsible for the system conceptualization, review and editing.

Data availability and materials

The dataset deployed/ analyzed during the current study are available from the corresponding author on reasonable request.

References

[1] Avsar Y, Fenercioglu A and Soyaslan M, "Design Optimization of PM Synchronous Motor: Rail Mounted Belt Drive Elevator Systems," IEEE TRANSACTIONS ON INDUSTRY APPLICATIONS, vol. 60, no. 1, pp. 301-311, 2024.

[2] Zhang Z and Xu B, "Research on the Application of Real Time Optimization Algoritm in improving the Intelligent Energy Consumption Control System of Elevator Transportation Efficiency," in 2024 IEEE 2nd International Conference on Electrical Automation and Computer Engineering (ICEACE), Changchun, China, 2024.

[3] Ctibor J and Pazdera I, "Comparison of the Common Control Techniques of Induction Machines," in 2018 IEEE International Conference on Environment and Electrical Engineering and 2018 IEEE Industrial and Commercial Power Systems Europe (EEEIC / I&CPS Europe), Palermo, Italy, 2018.

[4] Popov A, Lapshina V, Briz F and Gulyaev I, "Dynamic operation of FOC induction machines under current and voltage constraints," in 2017 19th European Conference on Power Electronics and Applications (EPE'17 ECCE Europe), Warsaw, Poland, 2017.

[5] Shabandokht-Zarami M, Ghanbari M, Alibeiki E and Jannati M, "IEEE CANADIAN JOURNAL OF ELECTRICAL AND COMPUTER ENGINEERING, VOL. 44, NO. 1, WINTER 2021 83 A Modified FOC Strategy With Optimal Rotor Flux for FTC of Star-Connected TPIMDs Against Single-Phase Open Fault," IEEE CANADIAN JOURNAL OF ELECTRICAL AND COMPUTER ENGINEERING, vol. 44, no. 1, pp. 83-93, 2021.

[6] Liu C and Luo Y, "Overview of Advanced Control Strategies for Electric Machines," Chinese Journal of Electrical Engineering , vol. 3, no. 2, pp. 53-61, September 2017.

[7] Ouanjli N, Derouich A, Ghzizal A, Chebabhi A and Taoussi M, "A comparative study between FOC and DTC control of the Doubly Fed Induction Motor (DFIM)," in 2017 International Conference on Electrical and Information Technologies (ICEIT), Rabat, Morocco, 2017.

[8] Ayana T, Kolodziejek P, Morawiec M and Wogi L, "Loss Minimization - Based Sensorless Control of High-Speed Induction Motor Considering Core Loss," IEEE Access, pp. 116341-116353, 2024.

[9] Cheng M, Zhou J, Qian W, Wang B, Zhao C and Han P, "Advanced Electric Motors and Control Strategies for High-quality Servo Systems - A Comprehensive Review," Chinese Journal of Electrical Engineering , pp. 63-85, 2024.

[10] Okpo E, E, Roux P. F and Nnachi A, "Induction Motor Fault Identification using Support Vector Machine," in 2023 6th International Conference on Renewable Energy and Power Engineering (REPE), Beijing, China, 2023.

[11] Barik L and Misra H, "Dual Side Field Oriented Control of Slip Ring Induction Motor," IEEE TRANSACTIONS ON INDUSTRIAL ELECTRONICS, pp. 15404-15414, 2024.

[12] Okpo E. E and I. E. Nkan I. E, "CONSTRUCTIONAL FEATURES AND PERFORMANCE ANALYSIS OF 3-PHASE LINEAR INDUCTION MOTOR," International Journal of Scientific Innovations and Sustainable Development, vol. 6, no. 1, pp. 176-185, 2016.

[13] Mehedi I. M, Saad N, M. A. Magzoub M. A, Al-Saggaf U. M and Milyani A. H, "Controllers, Simulation Analysis and Experimental Evaluation of Improved Field Oriented Controlled Induction Motors Incorporating Intelligent," IEEE Access, pp. 18380-18394, 2022.

[14] Kilic E, "Deep Reinforcement Learning-Based Controller for Field-Oriented Control of SynRM," IEEE Access, pp. 2855-2861, 2024.

[15] Zellouma D, Benbouhenni H, Bizon N and Bekakra Y, "A New Field-Oriented Control for Induction Motor Drive Using a Synergetic-Super Twisting Algorithm," in 2023 15th International Conference on Electronics, Computers and Artificial Intelligence (ECAI) , Bucharest, Romania, 2023.

[16] Jorge C, Electrical Machines Basic Theory, Adneli Consultant, S.L, 2021.

[17] Kolotilo V, Kulbashna N, Voronov R and Donets O, "The research of the elevator electromechanical system in terms of reducing the arising dynamic loads," in 2023 IEEE 4th KhPI Week on Advanced Technology (KhPIWeek), Kharkiv, Ukraine, 2023.

[18] Anh P. H, Kien C. V, Huan T. T and Khanh P. Q, "Advance Speed Control of PMSM Motors Using Neural FOC Method," in 2018 4th International Conference on Green Technology and Sustainable Development (GTSD), Ho Chi Minh City, Vietnam, 2018.

[19] Zhang M, Liu Y and Xu W, "Improved Torque Ripple Suppression Strategy for Brushless Doubly Fed Induction Generator-DC System Considering Winding Harmonic Loss," IEEE TRANSACTIONS ON POWER ELECTRONICS, vol. 39, no. 1, pp. 1209-1220, January 2024.

[20] Li W, Xu Z, Zhang and Yulin, "Induction motor control system based on FOC algoritm," in 2019 8th Joint International Information Technology and Artificial Intelligence Conference (ITAIC 2019), Zibo, China, 2019.

[21] Abunike C. E, Umoh G. D, Okpo E. E and Okoro O. I, "A Comparative Approach for the Analysis of Switched Reluctance Motors with Modified Rotor Pole Geometry," Nigerian Journal of Engineering, vol. 27, no. 3, pp. 2705-3954, 2020.

[22] Okpo E. E, Ogbonnaya I. O, Chukwuemeka C. A and Udochukwu B. A, "Investigating the Dynamic Behaviour of a Six Phase Induction Motor under Unbalanced Faults," in IEEE PES/IAS Power Africa, Nairobi, Kenya, 2020.